ACOUSTICS 2012

Quantitative ultrasonic tomography of high acoustic impedance contrast targets

R. Guillermin, P. Lasaygues and G. Rabau

Laboratoire de Mécanique et d'Acoustique, 31 chemin Joseph Aiguier, 13402 Marseille Cedex 20, France
guillermin@lma.cnrs-mrs.fr

This study is concerned with the ultrasonic imagery of elastic materials like cylinders or tubes by a diffraction tomography method. Green's representation is used to obtain an integral representation of the scattered field, and a discrete formulation of the inverse problem is obtained using a moment method. An iterative non-linear algorithm minimizing the discrepancy between the measured and computed scattered fields is used to reconstruct the sound speed profile in the target area. The minimization process is performed using a conjugated-gradient method. An experimental study with elastic targets immersed in water was performed. Cylindrical targets of various cross-sections have been selected. Inversions of experimental data are presented.

1 Introduction

This study focuses on the ultrasonic characterization and imaging of high impedance acoustical contrast targets. The aim is to obtain information about the shape, dimensions and sound speed profile of the studied object. In the case of high impedance contrast targets, ultrasonic wave propagation is greatly perturbed by the difference in the acoustic impedance between the scatterer and the surrounding medium (soft tissues, water or coupling gel). The aim of this work is then to solve this non-linear inverse scattering problem. Analytical or algebraic approaches may be applied generally involving in a problem of minimization of the differences between modeling data and measurements. Several strategies can be used to model the forward problem and to solve the inverse problem simply, efficiently and accurately. For many years, studies in the fields of ultrasound and electromagnetics have focused on directly solving the non-linear inverse scattering problem. Various methods have been presented in the literature, such as the Distorted Born Iterative Method [3][16][8][9] or the Contrast Source Method [19]. Experimental studies have been published in the electromagnetics domain [4][1][12] and interesting results have been obtained [2][5][7][13][6][18]. But as far as the authors know, few ultrasonic experimental results are available in literature [16][10][11] using non-linear inversion algorithms of this kind. The inversion method used in this study is based on the minimization, by a conjugated-gradient method, of a cost-function involving the discrepancy between the measured and computed scattered fields [13][14]. An experimental study was performed with cylindrical targets made of wax.

2 Description of the Inversion algorithm

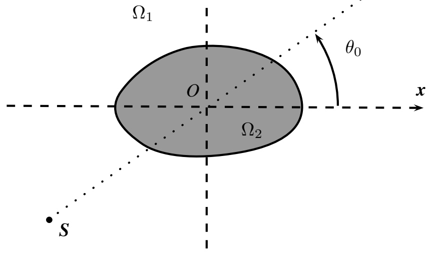

Figure 1: Geometry of the problem

Let us consider an inhomogeneous cylindrical (2D) object with an arbitrary cross section (occupying domain Ω_2) surrounded by an homogeneous medium (occupying Ω_1 (see figure 1)). Both media are fluid-like, linear and isotropic, c_1 and $c_2(\vec{X})$ are the sound speeds therein. The densities of the two media are assumed to be constant and equal. The object is illuminated by a monochromatic line source of frequency f placed at point $\vec{S}$: $P_0(\vec{X},t) = \Re(p^0(\vec{X})e^{-i\omega t})$ with $p^0(\vec{X}) = i/4H_0^1(k_1\|\vec{X}-\vec{S}\|)$ ($\omega = 2\pi f$ and $k_1 = \omega/c_1$). The time dependence $e^{-i\omega t}$ is dropped in the sequel. The total $p(\vec{X})$ and scattered $p^s(\vec{X})$ pressure fields can be expressed via the following integral representation:

$$p(\vec{X}) = p^0(\vec{X}) - k_1^2 \int_{\Omega_2} \Lambda(\vec{X}')p(\vec{X}')G_0(\vec{X}',\vec{X})\mathrm{d}\Omega(\vec{X}') \tag{1}$$

$$p^s(\vec{X}) = -k_1^2 \int_{\Omega_2} \Lambda(\vec{X}')p(\vec{X}')G_0(\vec{X}',\vec{X})\mathrm{d}\Omega(\vec{X}') \tag{2}$$

with $G_0(\vec{X},\vec{X}') = i/4H_0^1(k_1\|\vec{X}-\vec{X}'\|)$ the 2D free-field Green function and Λ the object function:

$$\Lambda(\vec{X}) = 1 - \frac{k^2(\vec{X})}{k_1^2} = 1 - \frac{c_1^2}{c_2^2(\vec{X})}$$

A discrete formulation of the integral representation is obtained by replacing the target by an array of $n \times n$ identical square cells each of which is small enough to assume Λ and p to be constant therein. Based on equations 1 and 2 we obtain:

$$p(\vec{X}) = p^0(\vec{X}) - k_1^2 \sum_{p=1}^{n}\sum_{q=1}^{n} \Lambda(\vec{X}_{pq})p(\vec{X}_{pq}) \int_{\Omega_{pq}} G_0(\vec{X},\vec{X}')\mathrm{d}\Omega(\vec{X}') \tag{3}$$

$$p^s(\vec{X}) = -k_1^2 \sum_{p=1}^{n}\sum_{q=1}^{n} \Lambda(\vec{X}_{pq})p(\vec{X}_{pq}) \int_{\Omega_{pq}} G_0(\vec{X},\vec{X}')\mathrm{d}\Omega(\vec{X}') \tag{4}$$

Using a collocation method in equation 3 we obtain for every point $\vec{X}_{ij}$ on the discretization grid:

$$p^0(\vec{X}_{ij}) = \sum_{p=1}^{n}\sum_{q=1}^{n} \left[\delta_{ip}\delta_{jq} + k_1^2\Lambda(\vec{X}_{pq}) \int_{\Omega_{pq}} G_0(\vec{X}_{ij},\vec{X}')\mathrm{d}\Omega(\vec{X}')\right] p(\vec{X}_{pq})$$

This equation can also be cast in matrix form:

$$P^0 = \left[I - G^D\left[\Lambda\right]\right] P$$

$$\text{with :} \quad P = \begin{bmatrix} p(\vec{X}_{11}) \\ \cdot \\ \vdots \\ p(\vec{X}_{nn}) \end{bmatrix} \quad \text{and} \quad P^0 = \begin{bmatrix} p^0(\vec{X}_{11}) \\ \cdot \\ \vdots \\ p^0(\vec{X}_{nn}) \end{bmatrix}$$

G^D is an $n^2 \times n^2$ operator depending on the surrounding medium Ω_1 and on the discretization grid. $[\Lambda]$ is a $n^2 \times n^2$ diagonal matrix containing the values of the contrast function at all points on the discretization grid.

Assuming that the scattered pressure field is known for M measurements points Y_j, equation 4 gives:

$$P^s = G^S\,[\Lambda]\,P,$$

where G^S is an $M \times n^2$ operator depending on the surrounding medium Ω_1, on the discretization grid and on the positions of the measurements points. The inverse scattering problem can then be written in the form of two coupled-equations [13]:

$$\begin{cases} P^s = G^s\,[\Lambda]\,P \\ P = \left[I - G^D\,[\Lambda]\right]^{-1} P^0 \end{cases},$$

that can be combined to form the error-function ρ giving the discrepancy between the measured and computed scattered fields:

$$\rho(\Lambda) = P^s - G^s\,[\Lambda]\left[I - G^D\,[\Lambda]\right]^{-1} P^0$$

Solving the inverse problem consists in minimizing the cost-function $J(\Lambda)$:

$$J(\Lambda) = \|\rho(\Lambda)\|^2$$

This kind of inverse problem is ill-posed and the stability of the algorithm is improve employing a Tikhonov regularization process.

The minimization of $J(\Lambda)$ is computed using the Polak-Ribière conjugate gradient process. Details on the implementation of the gradient procedure can be found in [13] [14].

3 Experimental study

3.1 Experimental Device

An experimental study was performed in a laboratory tank (see figure 3). Ultrasounds were generated using a pulser transmitter/receiver device and wide-band transducers. The nominal frequency of the transducers was 500 kHz and the usable bandwidth range from approximately 150 kHz to 750 kHz. Figure 2 shows an example of a transmitted time signal and its spectrum. The ultrasound Radio-Frequency (RF) received signals were digitized (14 bits, 20 MHz) using a data acquisition sheet.

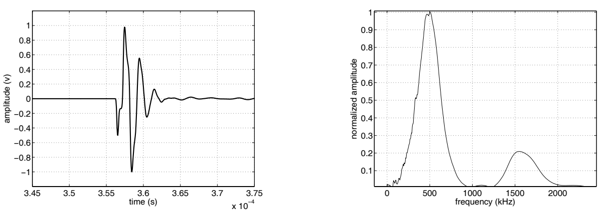

(a) (b)

Figure 2: Exemple of transmitted signal : (a) time signal, (b) spectrum

Ultrasonic measurements were performed in water at room temperature (18.4 C). The sector scanned was 360 degrees with both transducers with an angular increment of 10 degrees (36 x 36 signals). The transmitter and receiver described a circle around the target with a radius of 19 cm and 33 cm respectively (see figure 3).

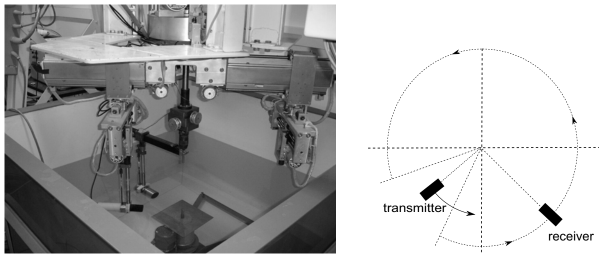

(a) (b)

Figure 3: Experimental set-up. (a): Ultrasound Scanner, (b): Configuration of the acquisitions

The experimental study was performed with two targets made of wax (A and B) described in figure 4. Target A is a cylinder with a 1.6 × 1.6 cm square cross-section. Target B is a cylinder with a 1.6 x 1.6 cm square cross-section with a circular cavity 5 mm in diameter. Both of these targets were immersed in water (one at a time). The cavity in target B was filled with water. The p-wave and s-wave sound speeds and attenuations were measured in wax samples. The acoustic parameters of the various media used are given in Table 1.

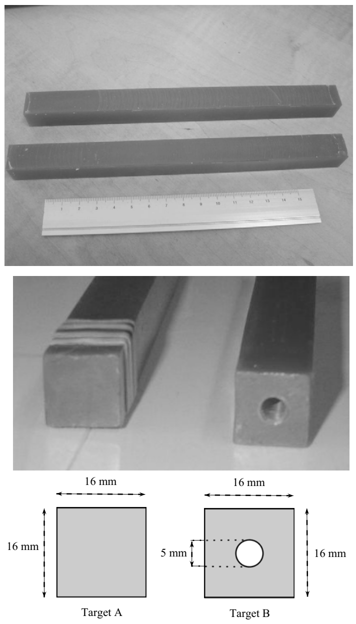

Figure 4: Description of targets

3.2 Inversion results

Figures 5 show the reconstructed p-wave sound speed for targets A and B. The frequency-hopping method was used [17][18][8] : iterations were performed by gradually increasing the working frequency with 4 frequencies chosen in the transducer bandwidth : 150kHz, 250kHz, 500 kHz and 750 kHz. In the case of

Table 1: Acoustic parameters of various media.

	water	wax
p-wave sound speed (m/s)	1477	2050
s-wave sound speed (m/s)	-	750
p-wave attenuation (Np/m/MHz)	-	55
s-wave attenuation (Np/m/MHz)	-	650

the iterations performed at 150 kHz, the background (water) was used as the initial guess in the iterative process. At other frequencies, the initial guess was the final result of the iteration process performed at the previous frequency. The iterative procedure was stopped when the norm of the relative variation of the contrast function between two steps of iteration was less than 0.5%.

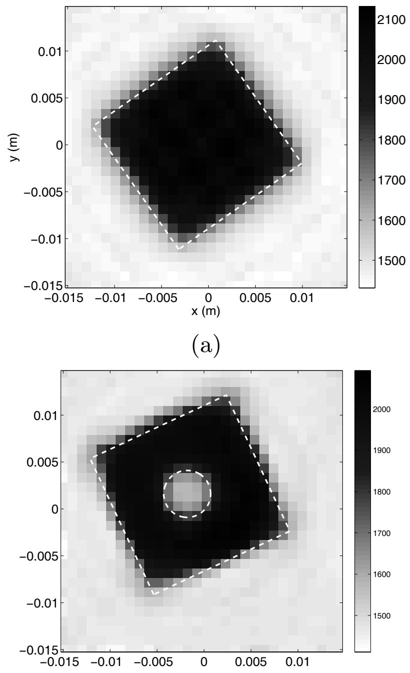

(a)

(b)

Figure 5: Results of the inversion of experimental data (the dashed line shows the actual target) for (a) : target A and (b) : target B

In both cases, the size and dimensions of the targets were accurately reconstructed : the relative error in the dimensions was about 15%. The p-wave sound speed was reconstructed with a relative error of 8%.

4 Conclusion

This paper deals with the two-dimensional imaging of a high-contrast target using a non-linear inversion method based on the minimization, using a conjugate-gradient algorithm, of a cost-function involving the discrepancy between the measured and computed scattered fields. An experimental study was performed with targets made of wax immersed in a water tank. The results obtained show that the non-linear inversion scheme can be used to accurately determine the shape, size and sound speed profile of the target (the error amounted to 8% in the p-wave sound speed and 15% in the dimensions).

References

[1] Belkebir K and Saillard M 2001 Special section: Testing inversion algorithms against experimental data *Inverse Problems* **17** 1565-1571

[2] Belkebir K and Tijhuis A G 2001 Modified gradient method and modified Born method for solving a two-dimensional inverse scattering problem *Inverse Problems* **17** 1671-1688

[3] Chew W C 1995 *Waves and fields in Inhomogeneous Media* (IEEE PRESS, New York)

[4] Coté M G 1992 Automated swept-Angle Bistatic scattering Measurements Using Continous Wave Radar *IEEE transactions on Instrumentation and Measurements* **41** 185-192

[5] Crocco L and Isernia T 2001 Inverse scattering with real data: detecting and imaging homogeneous dielectric objects *Inverse Problems* **17** 1573-1583

[6] Dubois A, Belkebir K and Saillard M 2005 Retrieval of inhomogeneous targets from experimental frequency diversity data *Inverse Problems* **21** S65-S79

[7] Duchene B 2001 Inversion of experimental data using linearized and binary specialized nonlinear inversion schemes *Inverse Problems* **17** 1623-1634

[8] Haddadin O S and Ebbini E S 1997 Multiple frequency distorted Born iterative method for tomographic imaging *Acoustical Imaging* **23** (Plenum Press)

[9] Haddadin O S and Ebbini E S 1998 Imaging strongly scattering media using a multiple frequency distorted Born iterative method *IEEE transactions on Ultrasonics , Ferroelectrics and Frequency Control* **45** 1485-1496

[10] Lasaygues P, Guillermin R, Lefebvre J-P 2006 Distorted Born diffraction tomography applied to inverting ultrasonic field scattered by noncircular infinite elastic tube *Ultrasonic Imaging* **28** 211-229

[11] Lavarello R Oelze M 2008 A Study of the Reconstruction of Moderate Contrast Targets Using the Distorted Born Iterative Method IEEE transactions on ultrasonics, ferroelectrics, and frequency control **55** 112-124

[12] Litman A and Crocco L 2009 Testing inversion algorithms against experimental data: 3D targets *Inverse Problems* **25** 020201

[13] Lobel P, Kleinman R, Pichot Ch, Blanc-Féraud L and Barlaud M 1996 Conjugated gradient method for solving inverse scattering with experimental data *IEEE Antennas & Propagation Magazine* **38** 48-51

[14] Lobel P 1996 Problèmes de diffraction inverse : reconstruction d'image et optimisation avec régularisation des discontinuités- Application à l'imagerie microonde *PhD Thesis* (University of Nice-Sohia Antipolis)

[15] Lobel P, Blanc-Féraud L, Pichot Ch and Barlaud M 1997 A New Regularization Scheme for Inverse Scattering *Inverse Problems* **13** 403-410

[16] Lu C, Lin J, Chew W and Otto G 1996 Image reconstruction with acoustic measurement using distorted Born iteration method *Ultrasonic Imaging* **18** 140-156

[17] Rekanos I T and Tsiboukis T D 1999 Inverse scattering using frequency-hopping *International Journal of Theoretical Electrotechnics* **7** 12-15

[18] Tijhuis A G, Belkebir K, Litman A C S and de Hon B P 2001 Multiple-frequency distorted-wave Born approach to 2D inverse profiling *Inverse Problems* **17** 1635-1644

[19] van den Berg P M and Kleinman R E 1997 A contrast source inversion method *Inverse Problems* **13** 1607-1620